# Enclosure 2

# MFN-09-395

# GEH Licensing Topical Report (LTR) "Reactor Internals Flow Induced Vibration Program, "NEDO-33259, Revision 2 – Public Version

HITACHI

3901 Castle Hayne Road
Wilmington, NC 28401

NEDO-33259
**Revision 2**
**Class I**
**eDRF-0000-0049-6672**
**June 2009**

**Licensing Topical Report**

# REACTOR INTERNALS FLOW INDUCED VIBRATION PROGRAM

## Legal Notice



## Proprietary Notice

## Acknowledgments

This document is the result of the technical contributions from many individuals and organizations in addition to the authors of this document. At the GE Hitachi Nuclear Energy (GEH), significant contributions to the development of BWR flow induced vibration technology has occurred over several decades. The names of these contributors are too numerous to list but are gratefully acknowledged here.

# TABLE OF CONTENTS

# LIST OF FIGURES

# LIST OF TABLES

# 1.0 INTRODUCTION

In Appendix 3L of the ESBWR Design Control Document (DCD), a process is described for evaluation of the ESBWR reactor internal components with respect to flow induced vibration (FIV). The purpose of this report is to provide the complete FIV evaluation of all reactor internals that includes both part 1 and part 2 as described by in Reference 1 except for the steam dryer, which will be evaluated in separate reports. This report provides additional details, for components that required additional work to evaluate and test for FIV, and to provide data for components that are considered acceptable and require no additional work. For those components where additional evaluation is being performed, the evaluation method, the results and conclusions are provided. For components requiring testing during the startup of the first ESBWR, the type and locations of sensors are identified. The plant that is used for comparison purposes that is closest to the ESBWR configuration is the Advance Boiling Water Reactor (ABWR). Three ABWR plants are currently in operation in Japan, and the first plant completed an FIV program that included analysis, testing and inspection as outlined in regulatory guide 1.20. Since the steam dryer FIV programs is covered in separate reports, this report focuses on the following components:

- Chimney Head/Steam Separator Assembly
- Shroud/Chimney Assembly
- Top Guide
- Core Plate
- Standby Liquid Control (SLC) piping
- Control Rod Drive Housings (CRDH)
- Control Rod Guide Tubes (CRGT)
- In-Core Monitor Guide Tubes (ICMGT)
- In-Core Monitor Housings (ICMH)
- Chimney and Chimney Partitions

The remaining reactor internal components that are not specifically identified in the referenced document, or in this report, are basically proven by past trouble-free BWR experience and have designs and flow conditions that are similar to prior operating BWR plants; e.g., the feedwater spargers and guide rods (guides, chimney assembly, chimney head and steam dryer in place during installation).

This report includes:

1. A list showing the locations and types of FIV sensors used in the ABWR FIV test (Table 1).
2. A list of similarities and differences between the ABWR and the ESBWR component design configurations (Table 2).
3. A determination of the ESBWR components natural frequencies based on the data from Table 2.

4. Data from the prototype ABWR FIV test that includes the lowest predicted natural frequencies of components, the dominant response frequencies during the FIV test, and the maximum zero-to-peak stress intensities calculated on the basis of strain gage measurements (Table 3).
5. Flow velocities in the ESBWR are compared to the ABWR (Table 3).
6. Comparison of the calculated ESBWR and ABWR lower plenum stresses (Table 4).
7. Assessments of the likelihood that FIV will not be an issue.
8. Detailed evaluation methodology, results, and conclusions for components requiring detailed evaluation.
9. Type and locations of sensors for monitoring FIV behavior during startup of the first ESBWR.

## 2.0 SUMMARY

Based on the evaluations performed in this report, the components that are evaluated in greater depth and will be part of the ESBWR FIV prototype test program are: the shroud/chimney assembly, the chimney head/steam separator assembly, the chimney, steam dryer and the SLC lines. The steam dryer will be evaluated in separate reports. For the remaining components, it has been concluded that no further evaluations are necessary since they are not susceptible to FIV. Due to the similarity of the ESBWR to the ABWR design, the ESBWR FIV program is considered to be non-prototype category II per Reference 2. Under this program, limited analysis and measurements of selected components is necessary, and full inspection of the reactor internals of the first plant is required.

# 3.0 DISCUSSION ON ABWR PROTOTYPE FIV TEST AND INSPECTION PROGRAM

The prototype ABWR reactor internals preoperational test program was performed in Japan. Although the program was carried out under the jurisdiction of the Japanese Ministry of International Trade and Industry (MITI), it also complied with the requirements of the U.S. Regulatory Commission (NRC) Regulatory Guide 1.20, Rev. 2 for a prototype design. Subsequent favorable operational experience has demonstrated structural adequacy of the ABWR reactor internals with respect to FIV. The program included analyses, measurements and inspections of reactor internals components deemed critical. Strain gages, accelerometers and linear variable differential transformer (LVDT) type relative displacement sensors were used for monitoring vibration levels. A total of [[ ]] sensors of different types were used to obtain vibration data on 11 different reactor internals component structures. The sensor locations were determined based upon the analytically predicted mode shapes for each structure, or in some cases, based upon the locations of past adverse inservice vibration phenomena. A variety of steady state and transient conditions that could be expected to occur during the life of the plant were included in the program. Test data were evaluated for five different testing conditions. The maximum zero to peak stress intensities calculated on the basis measurements during the ABWR startup FIV test program are shown in Tables 3 and 4.

The type of sensors, their locations and the basis for their locations are shown in Table 1.

# 4.0 GENERAL DISCUSSION OF REACTOR INTERNAL COMPONENT EVALUATIONS

## 4.1 Comparison of the ESBWR reactor internals component design to the ABWR design (Table 2).

A dimensional comparison of the ESBWR and the ABWR component designs is shown in Table 2. Also, see Figure 1, which shows the ABWR reactor pressure vessel with the reactor internals and Figure 2, which shows the same information for ESBWR. In general, the ABWR and ESBWR have the same components except that the ESBWR now includes a chimney, which has been added to increase natural circulation flow. Also, the fundamental flow paths within the ESBWR reactor vessel are essentially the same, but the flow path is now extended by the chimney. In addition to the inclusion of the chimney, the other major difference in the ESBWR reactor internals components design, compared to the ABWR design, is the standby liquid control piping (see Figure 3). Also, there are components that the ESBWR does not have such as the high pressure core flooder (HPCF) coupling or low pressure flooder (LPFL) spargers. The other traditional BWR components have dimensional differences that are shown in Table 2.

## 4.2 Comparison of ESBWR FIV behavior to ABWR (Table 3)

Table 3 shows the lowest predicted natural frequencies, the dominant response frequencies, and the maximum zero-to-peak stress intensities calculated on the basis of strain gage measurements made during the ABWR prototype FIV test. The data was extracted from the ABWR prototype FIV test report. Calculations based on the test results showed a maximum calculated zero-to-peak stress intensity of [[ ]]. This stress intensity is much less than the 68.9 MPa limit that is more conservative than the lowest $S_a$ value shown in the design fatigue curve for austenitic stainless steel, Figure I-9.2.1 of the ASME Code, Section III.

Table 3 also compares flow velocities that might induce vibrations due to vortex shedding from cylindrical components. The flow velocities were determined by using the geometry of the flow areas and coolant flow rates of [[ ]] for the ABWR and [[ ]] for the ESBWR. When calculating the flow velocities in the ESBWR RPV bottom head, [[ ]]. These maximum flow velocities were used to calculate the vortex shedding frequencies shown in Table 3.

Table 3 also shows the calculated natural frequencies of the ESBWR components. These calculations were performed using the natural frequencies reported for the ABWR as a reference basis to predict the ESBWR natural frequencies using classical formulas to account for the component geometry differences (dimensional analysis techniques).

# 5.0 SPECIFIC REACTOR INTERNAL COMPONENT EVALUATIONS

## 5.1 Chimney Head/Steam Separator Assembly

The ESBWR Chimney Head and Steam Separator assembly differs from earlier BWR designs in that the Chimney Head geometry is now flat compared to the domed shape on the traditional Shroud Head. Note that in the ESBWR, it is called a chimney head /steam separator assembly compared to prior BWR product lines, which have called it the shroud head/steam separator assembly, since the chimney is an additional component in ESBWR to which the head now attaches.

Additionally, the steam separator standpipes are longer, which will result in a lower natural frequency. Due to this change, the chimney head/steam separator assembly is selected for further evaluation. Restraints in the separator/standpipe "forest" are designed to increase the natural frequency and to minimize vibration responses to flow conditions. Accelerometers will be provided for the ESBWR prototype FIV test to confirm the adequacy of the design.

## 5.2 Shroud/Chimney Assembly

As shown in Figures 1 and 2, there are differences between the major components forming the ABWR core circulation path compared to the ESBWR design. For ABWR, the major core structure components, starting from the bottom attachment to the reactor pressure vessel (RPV), are the shroud support, shroud, top guide assembly, and the shroud head /steam separator assembly. These components form a complete assembly that is a freestanding structure, which has a full circumferential support between the RPV and the shroud. Also, there are bolted connections between the shroud and top guide assembly and also between the top guide assembly and shroud head/steam separator assembly.

In comparison to the ABWR, the ESBWR design has shroud support legs (12), shroud support ring, shroud, top guide, chimney, and chimney head/steam separator assembly. This assembly is also a freestanding structure; however, there are also eight lateral restraints at the top of the chimney structure that provide translational and torsional restraint that transmit loads through the RPV. Also, the support of the shroud involves the use of 12 support legs, each laterally braced, that provide a load path from the shroud to the RPV. For the ESBWR, there are bolted connections at the shroud to top guide, top guide to chimney, and chimney to chimney head.

The shroud/chimney/steam separator assembly is essentially an axisymmetric structure and the flow is also axisymmetric. Hence, no significant torsional excitation is expected. Any minor torsional forces from the non-axisymmetric structural elements, such as chimney internal partitions and separator structural ties, can be readily resisted by the lateral torsional restraints. Also, since the ESBWR flow is more uniform than the ABWR, any torsional fluid forces would be even smaller than in an ABWR. This more uniform flow behavior, in addition to the lateral torsional restraint at the top of the chimney, will result in an ESBWR torsional response that is less than the comparable ABWR response.

Because of the addition of the upper lateral restraint within the vessel, the ESBWR shroud/chimney calculated fundamental natural frequency is higher than that of the ABWR in spite of the ESBWR shroud/chimney/separator structure being taller. Table 5 shows that the fundamental frequency of the ABWR shroud/separator is [[ ]], while that of the ESBWR shroud/chimney/separator structure is [[ ]]. Because the flow velocity in the annulus between the RPV and the shroud for the ESBWR is higher due to a narrower annulus width, the pressure forces are also higher. Furthermore, due to the presence of the chimney, the total pressure force on the ESBWR shroud/chimney/separator structure is higher than that for the ABWR. These higher forces are partially compensated by the presence of the upper lateral restraint in the shroud/chimney/separator structure. In spite of the higher pressure forces, the calculated shroud/chimney/separator structure response is relatively small. Pertinent information comparing the ESBWR and ABWR shrouds, which supports the above statements, is shown in Table 5. Details of the analyses are provided below.

### 5.2.1 Shroud/Chimney Structure Dynamic Model and Response

Because of the essentially axisymmetric nature of the shroud chimney structure, the stiffening effects of the chimney/separator head, the top guide, and core plate, the shell modes of the shroud/chimney structure are greatly attenuated. Furthermore, the axisymmetric nature of the flow and related flow forces results in the beam response modes being dominant. Thus, a beam model of the structure is used to determine its FIV response. Two beam models, one for the ABWR and one for the ESBWR, have been created for comparison purposes. A comparison of the natural frequencies and dynamic responses of the ESBWR and the ABWR is provided in Table 5, which shows that the fundamental frequency of the ABWR shroud/separator is [[ ]], while that of the ESBWR shroud/chimney/separator structure is [[ ]].

To calculate the FIV response of ESBWR Shroud/Chimney/Separator structure, measured pressure time histories in the ABWR RPV-Shroud annulus were suitably scaled to define pressure time histories in the ESBWR RPV-Shroud/Chimney annulus. The scale factors were computed as the square of the ratio of ESBWR annulus fluid velocity to the corresponding value for the ABWR. Both the ABWR shroud and the ESBWR Shroud/Chimney structures were then analyzed using fluid forces resulting from the corresponding annulus pressure time histories to determine comparative responses of the Shroud/Chimney/Separator structure. During the prototype ABWR FIV test, the movement of the top guide was measured together with the shroud. The pressure time history was further normalized such that the calculated ABWR response would be equal to the measured ABWR response.

Using the results of these dynamic analyses, the accelerations and stresses at two locations along the shroud were obtained and are tabulated in Table 5. The ESBWR shroud stress is [[ ]] at the top guide elevation and is [[ ]] at the core plate elevation. These stresses are negligible compared to the allowable value of 68.9 MPa. The calculated forces and moments along the entire shroud/chimney/separator structure are used for calculating stresses as described below.

#### 5.2.1.1 FIV Stress Analysis Results and Evaluation

Using the forces and moments derived from the dynamic model, maximum bending stresses in the Chimney Head & Steam Separator Assembly were calculated. The maximum predicted stress, including a fatigue strength reduction factor of [[ ]], is [[ ]], which occurs in the standpipes at the Chimney Head end. The calculated alternating peak stress intensity due to vibratory loads, which are continually applied during normal operations, is limited to 68.9 MPa for stainless steel. Thus, it is concluded that the FIV stresses are well below allowable values.

5.2.1.2 ESBWR Shroud Support Legs

The forces and moments obtained from the time history dynamic response analyses of the shroud/chimney/separator structure were used for obtaining maximum bending stresses in the support legs. The value computed is [[ ]]Mpa, which is much below the allowable limit of 68.9 MPa. A similar calculation for shroud support leg lateral braces shows that the maximum stress in the braces is [[ ]]Mpa, which is even less that that in the legs.

### 5.2.2 ESBWR Startup Instrumentation

The ABWR shroud was instrumented with strain gages during the ABWR prototype FIV test. The movement of the shroud was measured with displacement sensors located on the OD of the top guide. For the ESBWR, [[ ]] accelerometers, [[ ]] apart, will be placed near the calculated maximum acceleration elevation to measure the radial and tangential motion of the shroud/chimney/separator assembly. The maximum acceleration location is near the separator support ring. In addition, [[ ]] additional accelerometers, [[ ]] apart, will be placed at the midpoint of the chimney to measure chimney motion. A summary description of these sensors is contained in Table 6.

## 5.3 Top Guide Assembly

The ESBWR top guide is made from a solid forging that is the same as the ABWR design in the arrangement and size of the cells. The thickness of the Top Guide is 152.4 mm. In the dynamic model of the RPV and Internals, the Top Guide was modeled as a spring-mass system to account for the potential effect of its own natural frequency for FIV response. The spring, which represents the lateral stiffness of the Top Guide, connects the node representing the Top Guide to the node on the shroud at the elevation of the Top Guide. The dynamic analysis of the RPV and Internals model, under fluid-induced loads, was performed to obtain the maximum force in the spring representing the Top Guide. This force was determined to be [[ ]] and used in a subsequent detailed stress analysis of the Top Guide. The subsequent resulting peak stress value is considerably lower than the allowable value of 68.9 MPa.

## 5.4 Core Plate Assembly

The ESBWR core plate assembly is a similar design to the ABWR and BWR/6. The ESBWR Core Plate is a 210 mm stiff structure. In the dynamic model of the RPV and Internals, the Core Plate, like the Top Guide, was modeled as a spring-mass system to account for the potential effect of its own natural frequency for FIV response. The spring, which represents the lateral stiffness of the Core Plate, connects the node representing the Core Plate to the corresponding node on the shroud at the elevation of the Core Plate. The dynamic analysis of the RPV and Internals model, under fluid-induced loads, was performed to obtain the maximum force in the spring representing the Core Plate. This force was determined to be [[ ]] and used in a subsequent detailed stress analysis of the Core Plate. The subsequent resulting peak stress is considerably lower than the allowable value of 68.9 MPa.

## 5.5 Standby Liquid Control (SLC) Lines

The SLC line is a new ESBWR component that is located in the down-comer flow region in the annulus between the RPV and the chimney. The design is shown in Figure 3. Since the configuration of the SLC line has a new geometry and a location within the RPV, this component is analyzed in detail (described below) and will be included in the ESBWR prototype FIV test program.

A finite element beam model of the SLC line was constructed and analyzed for FIV induced stresses (Reference 3). The SLC line is supported at six places: the top vertical segment is supported at the RPV at two places along its [[ ]] length; the horizontal circular segment by two symmetrically placed supports at the shroud; and the two vertical segments in the bottom [[ ]] length were supported at the shroud by one support in each segment.

The fundamental frequency of the SLC line was determined to be [[ ]], which is over [[ ]] times (and well separated from) the vortex shedding frequency of [[ ]] and, therefore, is of no concern.

The SLC piping in the annulus will be instrumented during startup of the first ESBWR. A summary description of these sensors is shown in Table 6.

## 5.6 Control Rod Drive Housings (CRDH), Control Rod Guide Tubes (CRGT), In-Core Monitor Housings (ICMH) and In-Core Monitor Guide Tubes (ICMGT)

From Table 3 it is seen that the calculated natural frequencies of the CRGTs, ICMHs and ICMGTs of the ESBWR are higher than those reported for the ABWR. That is because the CRGTs, ICMHs and ICMGTs of the ESBWR have shorter lengths and have the same diameters, wall thicknesses, and mass per unit length. The increase in natural frequency effectively moves these components away from the dominant response frequency recorded by the ABWR test, and the values are high enough that FIV is not a concern. These components are exposed to lower flow velocities, and the corresponding vortex shedding frequencies are approximately a factor of [[ ]] less than those in the ABWR. In comparing the calculated natural frequencies to the associated vortex shedding frequencies, the component natural frequencies are, in all cases, much higher than the corresponding vortex shedding frequency. Therefore, FIV will not be a concern. These results are consistent with BWR operating plant experience where no FIV problems have ever been found in the lower region of the reactor vessel.

Since the ABWR flow induced vibration test did not reveal any significant vibration of the CRGTs, ICMHs, and ICMGTs and the peak stress intensities were well below the ASME Code limits, these ESBWR components have no FIV issues. The calculation described below confirms this.

The stresses due to flow induced vibrations (FIV) of reactor internal structures are determined by their structural characteristics and the fluid forces acting on them. For the calculation of stresses, the structural characteristics are defined by the natural frequencies and mode shapes. In the case of the ABWR, these frequencies were obtained from finite element models and confirmed by startup test data. The structural characteristics of the ESBWR (geometry, solid and fluid mass distributions, material properties and boundary conditions) are, except for the overall length, identical to the ABWR. Since the structural natural frequencies are inversely proportional to the square of the overall length, the ESBWR frequencies can be derived from the corresponding ABWR frequencies by using the ratio of length squared. The corresponding normalized mode shapes will essentially be the same.

The stresses due to flow-induced vibrations of reactor internal structures are also determined by the fluid forces from coolant flow. The dominant excitations are from vortex shedding and flow turbulence. The key parameter characterizing these excitations is the coolant flow velocity.

These velocities are higher in the ABWR; however, for calculating the stresses in the ESBWR, these forces have conservatively been assumed to be the same.

The CRGT and ICMGT stresses in ESBWR can thus be calculated by geometrically scaling the corresponding ABWR stresses. The ESBWR stresses thus obtained are presented in Table 4 along with the other data used in the calculation. These stresses are about 50% of the ABWR stresses for both the CRGT and ICMGT/ICMH structures.

It is therefore concluded that the CRGTs, ICMHs and ICMGTs can be excluded from the ESBWR prototype FIV test program and no instrumentation will be installed.

Based on previous BWR/5 experience, the CRDHs were not included in the ABWR FIV test program. Since the ESBWR CRDHs are rigid structures that are welded to the RPV bottom head and have [[ ]] times higher natural frequencies due to their shorter lengths and lower flow velocity in the bottom head, there will be no FIV issues with the ESBWR CRDHs. Therefore, the ESBWR CRDHs will not be instrumented during the prototype FIV test.

### 5.6.1 Shroud Instrumentation During ESBWR Startup

Due to the addition of the chimney in the structure, the shroud/chimney/separator structure will be more heavily instrumented than the ABWR was. In addition to [[ ]] accelerometers, [[ ]] apart, placed at the calculated maximum ESBWR shroud/chimney/separator acceleration elevation and [[ ]] accelerometers, [[ ]] apart, placed at the midpoint of the chimney, [[ ]] additional strain gages will be placed at the maximum calculated stress locations. These [[ ]] strain gages will be placed on the shroud above the shroud upper support ring along the calculated principal stress directions at the highest stress point. A summary of these sensors is found in Table 6.

## 5.7 ESBWR Chimney

### 5.7.1 ESBWR Chimney Scaled Model Tests

Because the chimney structure is unique to the ESBWR, a series of tests to simulate chimney partition FIV characteristics during normal ESBWR operation was performed.

Three scaled model tests were performed: a 1/6 scale, a 1/12 scale and one almost full scale (References 4 and 5). The tests use a mixture of air and water to simulate two-phase flow inside the chimney. Air was supplied by a compressor and the water was supplied by a water pump. The air and water were combined in a mixer at the chimney inlet and flow through the simulated chimneys. After passing through the chimney, the air-water mixture is separated and the water returned to the storage tank, and the air is exhausted to the atmosphere. A total of twelve pressure sensors were installed at ten elevations on the simulated chimney. There were two pressure sensors installed at each of two elevations.

The two smaller scale models were used to investigate the effect of model size on the test results. The test results show that the magnitude of the pressure fluctuations tend to [[ ]]. The smaller scaled model tests were also used to investigate the effects of inlet air/water mixing conditions on the pressure measurements. The tests showed that the inlet mixing condition had little influence on the test results.

To investigate the correlation of pressure fluctuation between cells, the [[ ]]-scale flow channel [[ ]] was divided into four. Correlation of pressure fluctuation between cells was evaluated using the test data. The correlation coefficients are [[ ]]. Therefore, it is concluded that the pressure fluctuations in each cell is [[ ]].

### 5.7.2 Chimney FIV Response

Test results from the large-scale model show a maximum peak-to-peak pressure of [[ ]]. This test result is used to calculate the FIV stresses in the chimney partitions. For stress evaluations, a Finite Element Model (FEM) using ANSYS Version 5.6 with plate and solid 3 D elements was developed. The FEM was used to extract the eigenvalues. Eigenvalue analysis shows the lowest frequency of the chimney is [[ ]]. Since the pressure forcing function from the tests is dominant around [[ ]], the chimney structure responds statically.

To calculate FIV response, the peak test pressures of [[ ]] were applied uniformly on four sides in one cell and the opposite pressure applied in adjacent cells. The calculated response results show the maximum stress occurs [[ ]]. Using a fatigue strength reduction factor of 2 for welded joints from ASME Code Sec. III Table NG-3352-1, the maximum stress intensity is [[ ]], which is sufficiently below the allowable value of 68.9 MPa.

### 5.7.3 Chimney FIV Experience at the Dodewaard Plant.

Dodewaard was the first and only naturally circulating BWR with a chimney similar to the ESBWR, and the two-phase flow velocity and void fraction were similar to those of the ESBWR. The structural characteristics of the chimneys for ESBWR and Dodewaard are similar. The Dodewaard plant operated for more than 20 years without any reported FIV issues. This experience gives added confidence the ESBWR will operate reliably without FIV problems.

# 6.0 REFERENCES

1. 26A6642AN Rev. 4 DCD Appendix 3L "Reactor Internal Flow Induced Vibration Program".
2. Regulatory Guide 1.20, Comprehensive Vibration Assessment Program for Reactor Internals during Preoperation and Initial Startup Testing, Revision 3, March 2007.
3. ESBWR SLC Piping FIV Stress Analysis Report, CE-OG-0110, Rev. 1, June 2007.
4. Large-Scale Chimney Partition FIV Report, CE-OG-0115, Rev. 0, March 2007.
5. FIV Study Report on ESBWR Chimney, Hitachi Report CE-OG-0095, Rev. 1, November 2006.

**Table 1:**
**ABWR Prototype FIV Test sensor Types, Locations, and Location Basis**

| Equipment Item | Location on Equipment | Sensor Type | Basis for Location |
|---|---|---|---|
| [[ | | | |
| | | | |
| | | | |
| | | | |
| | | | |
| | | | |
| | | | |
| | | | |
| | | | |
| | | | |
| | | | |
| | | | |
| | | | |
| | | | |

**Table 1:**
**ABWR Prototype FIV Test sensor Types, Locations, and Location Basis**

| | | | |
|---|---|---|---|
| | | | |
| | | | |
| | | | ]] |

**Table 2:**
**Comparison of ESBWR Reactor Internals Component Design to ABWR**
**(All dimensions are in mm)**

| FEATURE | ABWR | ESBWR | Difference |
|---|---|---|---|
| **RPV** | | | |
| Nominal ID | [[ | | |
| Minimum ID | | | |
| | | | |
| **Shroud** | | | |
| Upper shell OD | | | |
| Lower shell OD | | | |
| Wall thickness upper shell | | | |
| Wall thickness lower shell | | | |
| Total height | | | |
| Height upper shell | | | |
| Upper flange OD | | | |
| Upper flange ID | | | |
| Upper flange height | | | |
| Upper flange width | | | |
| Lower flange OD | | | |
| Lower flange ID | | | |
| Lower flange height | | | |
| Lower flange width | | | |
| Core plate support OD | | | |
| Core plate support ID | | | |
| Core plate support height | | | |
| Core plate support width | | | |
| | | | |
| **Annulus RPV/Shroud** | | | |
| Upper width | | | |
| Lower width | | | |
| | | | |
| **Top Guide Assembly** | | | |
| Overall OD | | | |
| Overall thickness | | | |
| | | | |
| **Core Plate Assembly** | | | |
| Core plate OD | | | |
| Core plate rim ID | | | |

| Table 2: Comparison of ESBWR Reactor Internals Component Design to ABWR (All dimensions are in mm) | | | |
|---|---|---|---|
| **FEATURE** | **ABWR** | **ESBWR** | **Difference** |
| Core plate rim height | | | |
| Core plate thickness | | | |
| Overall height | | | |
| Beam thickness | | | |
| Beam height | | | |
| | | | |
| **Chimney/Shroud Head and Separators** | | | |
| Overall height | | | |
| Chimney/Shroud head OD | | | |
| Height cylindrical portion | | | |
| Chimney/Shroud head height | | | |
| Number of separators | | | |
| Separator height | | | |
| Separator OD | | | |
| Standpipe OD | | | |
| Standpipe maximum height | | | |
| Separator pitch | | | |
| Overall diameter of separators | | | |
| Distance lower guide ring from the bottom | | | |
| Distance upper guide ring from the bottom | | | |
| Thickness of dome or plate | | | |
| OD of upper and lower rings | | | |
| Thickness of upper and lower guide rings | | | |
| Width of upper and lower guide rings | | | |
| **ESBWR Chimney (ABWR Top Guide Shell)** | | | |
| Shell OD | | | |
| Shell ID | | | |
| Shell thickness | | | |
| Total height | | | |
| Upper flange OD | | | |
| Upper flange ID | | | |
| Upper flange width | | | |
| Lower flange OD | | | |
| Lower flange ID | | | |
| Lower flange cross section | | | |
| Lower flange height at OD | | | |
| Lower flange height at ID | | | |

| Table 2: Comparison of ESBWR Reactor Internals Component Design to ABWR (All dimensions are in mm) | | | |
|---|---|---|---|
| **FEATURE** | **ABWR** | **ESBWR** | **Difference** |
| | | | |
| **Chimney Partition** | | | |
| Upper flange OD | | | |
| Upper flange ID | | | |
| Lower flange OD | | | |
| Lower flange ID | | | |
| Upper and lower flange width | | | |
| Upper and lower flange thickness | | | |
| Partition thickness | | | |
| Partition height | | | |
| Partition pitch | | | |
| Total height partition | | | |
| | | | |
| **CRD Housing** | | | |
| OD | | | |
| Wall thickness | | | |
| Length inside reactor (Max. length at center location including stub tube) | | | |
| | | | |
| **Control Rod Guide Tube** | | | |
| OD | | | |
| Wall thickness | | | |
| Length | | | |
| **Feedwater Sparger** | | | |
| OD | | | |
| Wall thickness | | | |
| Length | | | |
| | | | |
| **ICM Housing (incl. guide tube and stub tube)** | | | |
| OD | | | |
| Wall thickness | | | |
| Length inside reactor (incl. guide tube and stub tube) | | | |
| | | | |
| **ICM Guide Tube** | | | |
| OD | | | |

**Table 2:**
**Comparison of ESBWR Reactor Internals Component Design to ABWR**
**(All dimensions are in mm)**

| FEATURE | ABWR | ESBWR | Difference |
|---|---|---|---|
| Wall thickness | | | |
| Length | | | |
| | | | |
| **Guide Rod** | | | |
| OD | | | |
| Wall thickness | | | |
| Total length upper and lower guide rod | | | |
| | | | |
| **Standby Liquid control Lines** | | | |
| -Upper vertical portion | | | |
| OD | | | |
| Wall thickness | | | |
| Approximate length | | | |
| - Header | | | |
| OD | | | |
| Wall thickness | | | |
| Approximate length | | | |
| - Lower vertical portion | | | |
| OD | | | |
| Wall thickness | | | |
| Approximate length | | | ]] |

**Table 3:**
**Comparison of ESBWR FIV Behavior to ABWR**

| | ABWR | | ESBWR | | ABWR | | | ESBWR |
|---|---|---|---|---|---|---|---|---|
| Component | Lowest analytically predicted natural frequency (Hz) | Flow velocity m/sec | Natural frequency based on ABWR calculations (Hz) | Flow velocity m/sec | Dominant response during flow test (Hz) | Maximum zero to peak stress intensity calculated on the basis of strain gage measurements during flow test. Limit is 68.9 MPa (7.0 kg/mm²) | Calculated vortex Shedding Frequency (Hz) | Calculated vortex Shedding Frequency (Hz) |
| Shroud | [[ | | | | | | | |
| Chimney | | | | | | | | |
| Top Guide | | | | | | | | |
| Control Rod Guide Tube | | | | | | | | |
| In-core Housings | | | | | | | | |
| In-core Guide Tubes | | | | | | | | |
| CRD Housings | | | | | | | | ]] |

**Table 4:**
**Calculation of ESBWR Component Maximum Stresses From ABWR Data.**

| Component | Length (mm) | | Lowest Analytically Predicted Natural Frequency (Hz) (See Note 1 Below) | | Calculated Vortex Shedding Frequency (Hz) | | Maximum (0-Peak) Stress Intensity on the Basis of Strain Gage Measurements During Flow Test. (MPa / kg/mm$^2$) | Predicted Maximum Stress Intensity (MPa / kg/mm$^2$) (Note 3) |
|---|---|---|---|---|---|---|---|---|
| | ABWR | ESBWR | ABWR | ESBWR | ABWR | ESBWR | ABWR | ESBWR |
| Control Rod Guide Tube | [[ | | | | | | | |
| CRD Housing | | | | | | | | |
| In-Core Guide Tubes | | | | | | | | |
| In-Core Housing (including ICGT) | | | | | | | | |

]]

| Table 5: Comparison of ESBWR and ABWR Shroud/Separator FIV Response | | |
|---|---|---|
| **Response Quantity** | **ABWR** | **ESBWR** |
| Shroud First Lateral Frequency | [[ | |
| Shroud Stress at Top Guide Elevation | | |
| Shroud Stress at Core Support Elevation | | |
| Shroud Horizontal Acceleration at Top Guide Elevation | | |
| Top Guide Mass Acceleration | | |
| Shroud Horizontal Acceleration at Core Support Elevation | | |
| Core Plate Mass Acceleration | | |
| Top Guide 'Spring' Force | | |
| Core Support Plate 'Spring' Force | | ]] |

[[

]]

| Table 6: ESBWR Prototype FIV Test Sensor Types, Locations, and Location Basis | | | |
|---|---|---|---|
| **Equipment Item** | **Location on Equipment** | **Sensor Number and Type** | **Basis for Location** |
| [[ | | | |
| | | | |
| | | | |
| | | | |
| | | | ]] |

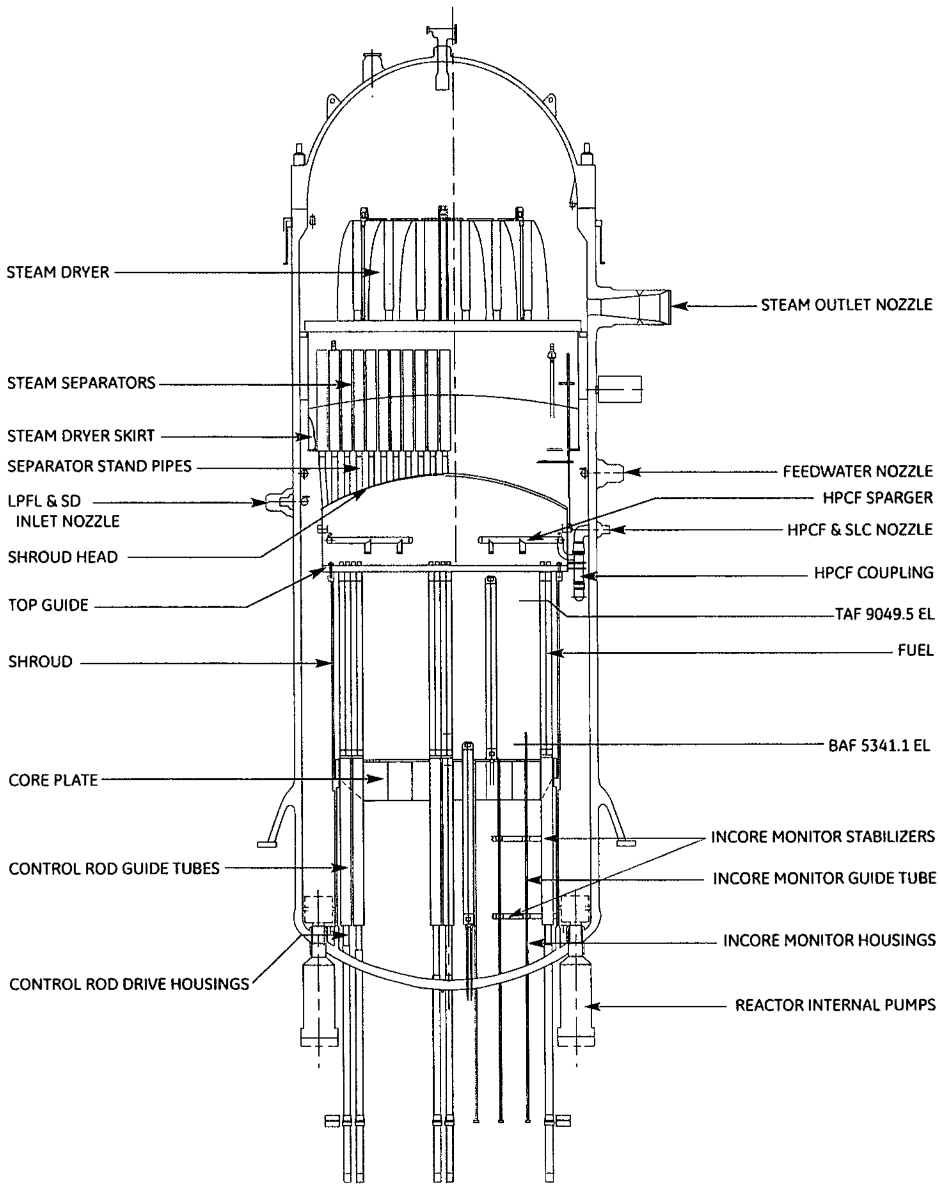


**Figure 1. ABWR RPV Assembly**

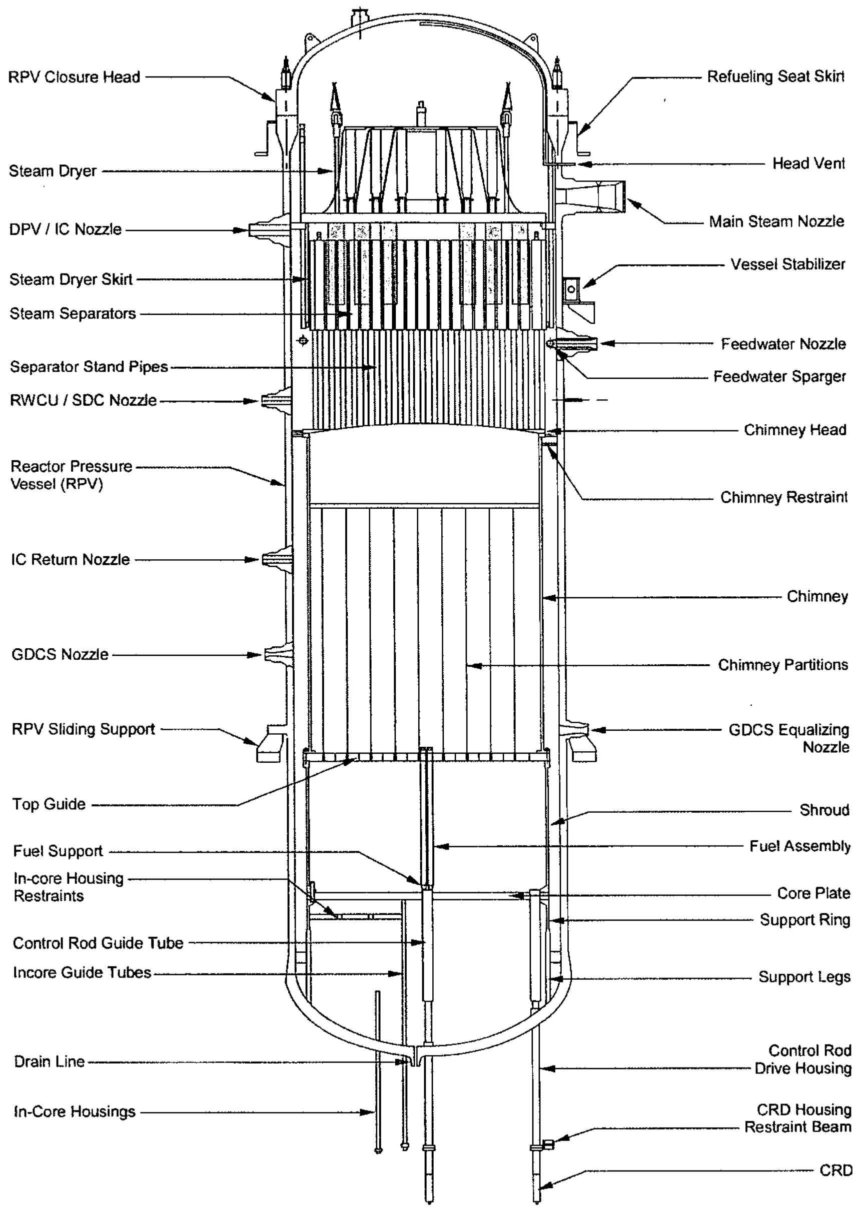


**Figure 2. ESBWR Reactor Assembly**

[[

]]

**Figure 3. ESBWR Standby Liquid Control Injection Piping/Headers and Nozzles**

end of document

Total page count 32

**MFN 09-395**

**Enclosure 3**

**Affidavit**

# GE-Hitachi Nuclear Energy Americas LLC

## AFFIDAVIT

**I, David H. Hinds,** state as follows:

(1) I am the Manager, New Units Engineering, GE Hitachi Nuclear Energy ("GEH"), have been delegated the function of reviewing the information described in paragraph (2) which is sought to be withheld, and have been authorized to apply for its withholding.

*(2)* The information sought to be withheld is contained in Enclosure 1 of GEH letter MFN 09-395, Mr. Richard E. Kingston to U.S. Nuclear Regulatory Commission, entitled *Transmittal of GEH Licensing Topical Report (LTR) "Reactor Internals Flow Induced Vibration Program," NEDE-33259P, Revision 2 and NEDO-33259, Revision 2,* dated June 11, 2009. The GEH proprietary information in Enclosure 1, which is entitled *Reactor Internals Flow Induced Vibration Program, NEDE-33259P, Revision 2 - Proprietary Version* is delineated by a [[dotted underline inside double square brackets.{3}]]. Figures and large equation objects are identified with double square brackets before and after the object. In each case, the superscript notation {3} refers to Paragraph (3) of this affidavit, which provides the basis for the proprietary determination. A non-proprietary version of this information is provided in Enclosure 2, *Reactor Internals Flow Induced Vibration Program, NEDO-33259, Revision 2 - Public Version.*

(3) In making this application for withholding of proprietary information of which it is the owner, GEH relies upon the exemption from disclosure set forth in the Freedom of Information Act ("FOIA"), 5 USC Sec. 552(b)(4), and the Trade Secrets Act, 18 USC Sec. 1905, and NRC regulations 10 CFR 9.17(a)(4), and 2.390(a)(4) for "trade secrets" (Exemption 4). The material for which exemption from disclosure is here sought also qualify under the narrower definition of "trade secret," within the meanings assigned to those terms for purposes of FOIA Exemption 4 in, respectively, Critical Mass Energy Project v. Nuclear Regulatory Commission, 975F2d871 (DC Cir. 1992), and Public Citizen Health Research Group v. FDA, 704F2d1280 (DC Cir. 1983).

(4) Some examples of categories of information which fit into the definition of proprietary information are:

a. Information that discloses a process, method, or apparatus, including supporting data and analyses, where prevention of its use by GEH competitors without license from GEH constitutes a competitive economic advantage over other companies;

b. Information which, if used by a competitor, would reduce his expenditure of resources or improve his competitive position in the design, manufacture, shipment, installation, assurance of quality, or licensing of a similar product;

c. Information which reveals aspects of past, present, or future GEH customer-funded development plans and programs, resulting in potential products to GEH;

d. Information which discloses patentable subject matter for which it may be desirable to obtain patent protection.

The information sought to be withheld is considered to be proprietary for the reasons set forth in paragraphs (4)a., and (4)b, above.

(5) To address 10 CFR 2.390(b)(4), the information sought to be withheld is being submitted to NRC in confidence. The information is of a sort customarily held in confidence by GEH, and is in fact so held. The information sought to be withheld has, to the best of my knowledge and belief, consistently been held in confidence by GEH, no public disclosure has been made, and it is not available in public sources. All disclosures to third parties including any required transmittals to NRC, have been made, or must be made, pursuant to regulatory provisions or proprietary agreements which provide for maintenance of the information in confidence. Its initial designation as proprietary information, and the subsequent steps taken to prevent its unauthorized disclosure, are as set forth in paragraphs (6) and (7) following.

(6) Initial approval of proprietary treatment of a document is made by the manager of the originating component, the person most likely to be acquainted with the value and sensitivity of the information in relation to industry knowledge, or subject to the terms under which it was licensed to GEH. Access to such documents within GEH is limited on a "need to know" basis.

(7) The procedure for approval of external release of such a document typically requires review by the staff manager, project manager, principal scientist or other equivalent authority, by the manager of the cognizant marketing function (or his delegate), and by the Legal Operation, for technical content, competitive effect, and determination of the accuracy of the proprietary designation. Disclosures outside GEH are limited to regulatory bodies, customers, and potential customers, and their agents, suppliers, and licensees, and others with a legitimate need for the information, and then only in accordance with appropriate regulatory provisions or proprietary agreements.

(8) The information identified in paragraph (2), above, is classified as proprietary because it identifies detailed GE ESBWR design information. GEH utilized prior design information and experience from its fleet with significant resource allocation in developing the system over several years at a substantial cost.

The development of the evaluation process along with the interpretation and application of the analytical results is derived from the extensive experience database that constitutes a major GEH asset.

(9) Public disclosure of the information sought to be withheld is likely to cause substantial harm to GEH's competitive position and foreclose or reduce the availability of profit-making opportunities. The information is part of GEH's comprehensive BWR safety and technology base, and its commercial value extends beyond the original development cost. The value of the technology base goes beyond the extensive physical database and analytical methodology and includes development of the expertise to determine and apply the appropriate evaluation process. In addition, the technology base includes the value derived from providing analyses done with NRC-approved methods.

The research, development, engineering, analytical and NRC review costs comprise a substantial investment of time and money by GEH.

The precise value of the expertise to devise an evaluation process and apply the correct analytical methodology is difficult to quantify, but it clearly is substantial.

GEH's competitive advantage will be lost if its competitors are able to use the results of the GEH experience to normalize or verify their own process or if they are able to claim an equivalent understanding by demonstrating that they can arrive at the same or similar conclusions.

The value of this information to GEH would be lost if the information were disclosed to the public. Making such information available to competitors without their having been required to undertake a similar expenditure of resources would unfairly provide competitors with a windfall, and deprive GEH of the opportunity to exercise its competitive advantage to seek an adequate return on its large investment in developing these very valuable analytical tools.

I declare under penalty of perjury that the foregoing affidavit and the matters stated therein are true and correct to the best of my knowledge, information, and belief.

Executed on this 11th day of June, 2009.

David H. Hinds
GE-Hitachi Nuclear Energy Americas LLC